

MuCoMiD: A Multitask graph Convolutional Learning Framework for miRNA-Disease Association Prediction

Ngan Dong¹, Stefanie Mücke², Megha Khosla¹

¹ L3S Research Center, Leibniz University of Hannover, Hannover, Germany

² TRAIN Omics, Translational Alliance in Lower Saxony, Hannover, Germany

Email: dong@l3s.de

Abstract—Growing evidence from recent studies implies that microRNA or miRNA could serve as biomarkers in various complex human diseases. Since wet-lab experiments are expensive and time-consuming, computational techniques for miRNA-disease association prediction have attracted a lot of attention in recent years. Data scarcity is one of the major challenges in building reliable machine learning models. Data scarcity combined with the use of precalculated hand-crafted input features has led to problems of overfitting and data leakage.

We overcome the limitations of existing works by proposing a novel multi-tasking graph convolution-based approach, which we refer to as MuCoMiD. MuCoMiD allows automatic feature extraction while incorporating knowledge from five heterogeneous biological information sources (interactions between miRNA/diseases and protein-coding genes (PCG), interactions between protein coding genes, miRNA family information, and disease ontology) in a multi-task setting which is a novel perspective and has not been studied before. To effectively test the generalization capability of our model, we construct large-scale experiments on standard benchmark datasets as well as our proposed larger independent test sets and case studies. MuCoMiD shows an improvement of at least $\sim 3\%$ in 5-fold CV evaluation on HMDDv2.0 and HMDDv3.0 datasets and at least $\sim 35\%$ on larger independent test sets with unseen miRNA and diseases over state-of-the-art approaches. We share our code for reproducibility and future research at <https://git.l3s.uni-hannover.de/dong/cmtd>.

Index Terms—graph representation learning, multitask, data integration, miRNA, disease



1 INTRODUCTION

Beginning in the early 2000s, the biological dogma that proteins are responsible for most functions in a cell began to shift and new classes of non-coding, regulatory RNAs became points of interest. The highly conserved class of microRNAs (miRNAs) with an approximate length of 22 nucleotides were first considered “junk” DNA without function and emerged as regulators in cell development, maturation, differentiation, and apoptosis of the cell, cell signaling, cellular interactions, and homeostasis [1], [2], [3].

MicroRNAs fulfill their diverse functions by regulating gene expression of protein-coding genes (PCGs) after transcription. The transcribed mRNA of PCGs can be directly bound by miRNAs, which leads to cleavage or destabilization of the mRNA and represses the translation into proteins [4]. Each miRNA can have hundreds of target mRNAs and mRNAs can be regulated by more than one miRNA, resulting in complex networks that are yet to be fully understood. The mutation of miRNAs or changes in their expression can have widespread consequences that can be hard to predict.

Consequently several associations between miRNAs and diseases have been confirmed using biological experiments leading to the belief that miRNAs could be potential biomarkers in certain diseases such as cancers or immune-related diseases [5], [6], [7], [8], [9], [10], [11]. Besides unveiling a deeper understanding of diseases’ molecular pathogenesis, identifying potential associations between miRNAs

and diseases can also help in the treatment and discovery of possible drug targets.

Owing to the significance of the problem and the time-consuming nature of biological experiments, recent years have seen an upsurge in machine learning approaches [12], [13], [14], [15], [16] for *predicting miRNA-disease associations*. Being successfully able to predict miRNA-disease associations can lead to information prioritisation in biological wet-lab experimentation, which will result in considerable time and cost savings. From a machine learning perspective, the problem of predicting miRNA-disease associations can be formulated as that of a *link prediction problem* in a bipartite graph, where miRNA and disease form the two sets of nodes. However, as is typical to many biomedical applications, a major challenge for building generalizable and eventually well-performing models for the miRNA-disease association prediction problem is *data scarcity* of miRNA-disease data. For example, the total number of miRNA and disease nodes (without any preprocessing and removal of duplicates) in the standard HMDD v2.0 [17] database are 495 and 383 respectively with a total of 5,430 associations (links). These networks are therefore not only small with respect to the nodes set but are also sparsely connected.

Data scarcity often leads to biased and non-generalizable models. Earlier attempts to address data scarcity rely on creating additional secondary features based on the initial feature set by computing intra-node similarities, e.g.,

miRNA functional similarity. So much so, that these secondary features that encode miRNA functional similarity are pre-computed and are even deposited in well-known databases like MISIM [18]. The first problem associated with using such similarity-based input features is that it is prone to overfitting because slight errors in the input features get amplified by the secondary features. Secondly, models based on secondary features cannot be used to predict new associations for a miRNA (or a disease), i.e., instances for which no prior disease (or miRNA) association information is available.

More worrying is the problem of *data leakage* when using pre-computed miRNA functional similarities indiscriminately from available databases. Dong and Khosla [19] find that most of the existing works that employ pre-computed similarities in model building ignore the actual train/test split giving rise to *data leakage*. In other words, some of the associations which are to be tested by the model are already present in the association network that was used to compute the similarity features. Finally, the small dataset size for the miRNA-disease prediction task prohibits the utility of flexible and more expressive modern representation learning approaches.

1.1 Present work

We overcome the above limitations in the earlier literature by avoiding the creation of secondary features altogether. Instead, our approach attempts to address the data scarcity problem by integrating knowledge from multiple heterogeneous sources of information available for miRNA and diseases in addition to the miRNA-disease associations. Combining multiple data sources enables us to compensate for missing or unreliable information in any single data type leading to more reliable predictions. Our key contribution is to model the integration of heterogeneous knowledge sources into a common representation space that can be trained end-to-end using modern representation learning machinery.

To this end, we propose a **Multitask graph Convolutional neural network for miRNA-Disease association prediction**, which we refer to as MUCOMID for brevity. MUCOMID allows automatic feature extraction while incorporating knowledge from five heterogeneous biological information sources (interactions between miRNA/diseases and protein-coding genes (PCG), interactions between protein-coding genes, miRNA family information, and disease ontology) in a *multi-task setting*. Instead of pre-calculated secondary features for miRNA and disease as in previous works, we employ graph convolution operation (without the non-linear activation) over the corresponding biological networks to learn informative representations for miRNA and disease automatically at training time. Overall we have an expressive linear model with non-linear activation only at the output layer.

The added side tasks serve as regularizers and help us to incorporate domain-knowledge. For example, an miRNA m regulates a set of proteins p that are responsible for some biological functions. Moreover, disruptions in the biological functions of p lead to certain disease condition d . Then m has some influence over disease d via p . The

additional tasks of predicting miRNA-PCG interaction and disease-PCG interaction help us to encode such influence by embedding m and d closer in the representational space. Besides, we employ *adaptive loss balancing* techniques to fine-tune multi-task loss gradients. This allows us to utilize the full power of multi-task learning without resorting to exhaustive hyperparameter search.

We conduct an extensive evaluation of our approaches in comparison to earlier works on existing benchmark datasets retrieved from HMDD v2.0 [17] and HMDD v3.0 [20] databases. In addition to standard benchmark datasets, we also construct and test on new and larger independent test sets. We finally present case studies for three specific diseases to showcase the utility of our approach in predicting the association of novel diseases for which no prior miRNA association information is available in the train set.

Our Contributions. To summarize, we make the following contributions:

- We model the miRNA-disease association prediction problem in a *multi-task setting* incorporating heterogeneous domain knowledge, which is a novel perspective and has not been studied before for the current problem.
- We construct four new larger test sets for testing in transductive (when miRNA and disease nodes in the test set are also present in the train set) and inductive settings (when the test set contains a number of new miRNA or disease nodes).
- We conduct large-scale experiments, ablation study and case studies for three specific diseases to showcase the superiority of our approach.
- We release all the code and data used in this work for reproducibility and future research at <https://git.l3s.uni-hannover.de/dong/cmtd>.

2 PROBLEM STATEMENT AND RELATED WORK

The miRNA-disease association data can be represented using a bipartite graph $\mathcal{G}_{md} = (M, D, E)$ where M is the set of nodes representing miRNAs and D denotes the set of disease nodes. Each edge $e = (m, d) \in E$ denotes the association between the miRNA node m and disease node d . We are then interested in the following problem statement.

Problem statement Given the bipartite graph $\mathcal{G}_{md} = (M, D, E)$, we are interested in (i) predicting missing links among the given nodes (*transductive setting*) (ii) predicting new links for so far unseen novel miRNA or disease nodes (*inductive setting*).

2.1 Related work

Existing computational approaches for miRNA-disease association prediction can be broadly grouped into three classes: *scoring-based*, *network topology* and *machine learning based methods*.

Assuming that the miRNA pairs linked to common diseases are functionally more related scoring based methods [18], [21] proposed scoring systems to prioritize miRNA-disease associations. A more sophisticated scoring scheme while integrating information from miRNA and disease

similarity networks was proposed in [22]. Network based approaches [23], [24], [25] construct miRNAs and/or disease similarity networks and aims at efficiently transferring known miRNA-disease association labels between similar miRNAs and/or similar diseases in the network. Chen et al. [23] employ repeated random walks with restarts over the miRNA functional similarity network and prioritize candidate miRNA-disease associations using the final stable walk probability.

More closely related to our work is the third category of machine learning based methods. Approaches in this category mainly rely on using secondary or hand-crafted features to construct similarity networks from which latent node features are extracted using graph-based representation learning techniques. EPMDA [12] extracts edge perturbation-based features from the miRNA-disease heterogeneous network and then trains a Multilayer Perceptron regression model to prioritize miRNA-disease associations. NNMDA [26] combines information from five different miRNA similarities and two disease similarities to build a heterogeneous network for feature learning and association prediction. [27] incorporates information from multiple domains, for example, miRNA-lncRNA and miRNA-PCG interaction, miRNA-drug association, disease-lncRNA, disease-PCG association, disease-drug association, to build a heterogeneous information network for feature extraction. The graph-based features along with miRNA k-mer feature (calculated from the miRNA sequence) and disease semantic similarity are concatenated to form the input to a Random Forest classifier for association prediction.

Another line of works include NIMGCN [16] and DimiG [15] which propose end-to-end learning approaches in which graph convolution networks (GCNs) [28] are employed for extracting latent features of miRNA and disease nodes. Non-graph based approaches like DBMDA [13] extract latent features from input hand-crafted features consisting of miRNA functional, disease semantic, and miRNA sequence similarity using autoencoders. The latent features are then fed to a Rotation Forest [29] classifier.

The reliance on hand-crafted features based on existing association data limits the applicability of existing techniques to transductive settings. Hence, apart from other limitations with respect to model generalization and data leakage (already discussed in Section 1) a majority of these approaches cannot be applied to predict associations for new miRNA or disease nodes that have not been observed in training data.

3 PROPOSED APPROACH

Given the input bipartite miRNA-disease network \mathcal{G}_{md} , we treat the miRNA-disease association problem as a binary classification where the label for an input pair node (m, d) is 1 if there is a known association between them and 0 otherwise.

To overcome the challenges of data scarcity, we propose MUCOMID in which we focus on *effectively integrating heterogeneous biological information while learning to predict missing or new miRNA-disease associations*. Instead of relying on secondary or handcrafted features, we rely on other

knowledge sources to learn the input representation automatically at training time. Also recent works indicate that PCGs are the most important link between miRNAs and their associated diseases [30] since changes in miRNAs lead to differently regulated PCGs, which in turn can cause diseases. Therefore, in addition to the miRNA-disease association prediction task (formulated as a binary classification problem), we add miRNA-PCG and disease-PCG interaction confidence score prediction (formulated as regression tasks) as two additional side tasks to incorporate additional domain knowledge and prevent overfitting.

In summary, MUCOMID employs different ways of integrating domain knowledge at different stages of the model building process. In particular, information from three different biological networks namely, miRNA family, PCG-PCG interaction, and disease ontology is directly used as inputs to learn the node representations during training. Besides, the miRNA-PCG and disease-PCG interactions are employed to build additional regularization objective functions. The incorporation of various information sources help compensate for the lack of information in single data source. It also helps in mitigating the data scarcity problem.

In the following we describe the three modules of MUCOMID (also depicted in Figure 1): (i) *input graph construction*, (ii) *graph convolution based feature extraction*, and (iii) *multi-task optimization/learning*.

3.1 Input graph construction

We start by describing the construction or retrieval of various biological networks that we leverage as additional sources of information and the corresponding rationale.

miRNA family, \mathcal{G}_m . A miRNA family is the group of miRNAs that share a common ancestor in the phylogenetic tree. miRNAs that belong to the same family usually have highly similar sequences, secondary structures and tend to execute similar biological functions [31]. Similar miRNA would tend to participate in the mechanisms of similar diseases. We retrieve miRNA family information from mirBase database [32]. The miRNA network \mathcal{G}_m is an unweighted undirected graph in which there is a connection between node A and node B if A and B belong to the same family. Figure 2 presents an illustration of the miRNA family network generated from our data.

Disease ontology, \mathcal{G}_d . The disease ontology [33] represents the disease etiology classes. A directed connection between two diseases exists if there exists a **is-a** relationship between them. Similar diseases can be expected to interact with similar miRNAs. The disease ontology network \mathcal{G}_d is an unweighted directed network in which there is a directed connection from A to B if B is a parent of A. \mathcal{G}_d can be visualized as a directed tree which contains only directed connection between children and parents nodes. Each tree layer represents one layer of abstraction. The upper most layer represents the most general disease category. An illustration of the disease ontology is given in figure 3.

PCG-PCG interaction, \mathcal{G}_p . PCGs interact with PCGs to carry out biological functions. Therefore, given the fact that protein coding gene p_1 activates the expression of protein coding gene p_2 , if the miRNA m can regulate p_1 then there

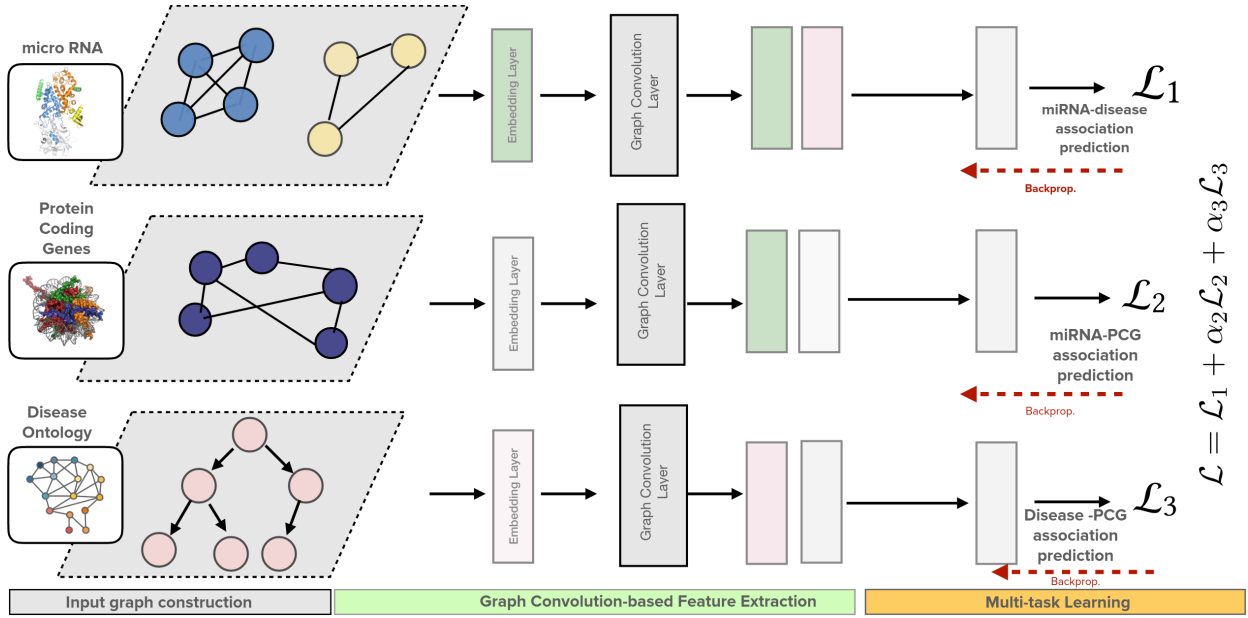


Fig. 1. A schematic diagram of MuCoMID. MuCoMID consists of three main modules: (i) input graph construction in which we build networks corresponding to the available side information from miRNA family, PCG-PCG interactions, and disease ontology (ii) the second module takes the constructed networks as input and generates the nodes' representation according to their local neighbors (iii) finally, one classifier for miRNA-disease association prediction, two regressors for miRNA-PCG and disease-PCG interaction confidence score prediction are added. The second and third modules get trained jointly using a multitask loss. The multitask loss is a weighted sum of the three individual task losses and is optimized using a *dynamic loss balancing* technique.

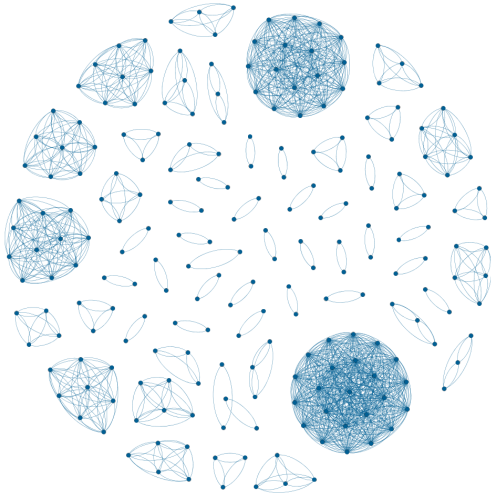


Fig. 2. An illustration of the miRNA family network.

should be some relation between m and p_2 . In other words, information from the protein-protein interaction network will bring additional insights about indirect relationship between miRNAs/diseases and the rest of PCGs with which a direct interaction is not known. An example of the miRNA-PCG, PCG-PCG interactions is presented in figure 4 where red nodes and red edges denote miRNAs and miRNA-PCG connections while blue nodes and blue edges represent PCGs and PCG-PCG interactions, respectively. We download PCG interaction data from STRING v10 database [34]. As preprocessing step, we retain only interactions between PCGs that have at least one known interaction with miRNAs

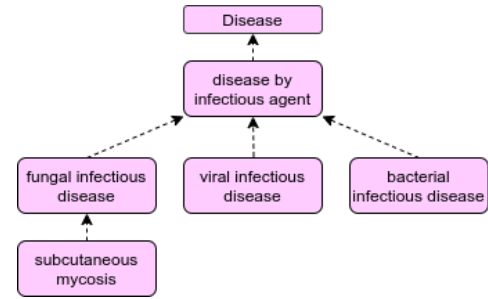


Fig. 3. An illustration of the disease ontology. Directed edges denote 'is_a' relations

or diseases. The PCG network \mathcal{G}_p is an undirected weighted network in which the edge weights correspond to the confidence score of PCG-PCG interaction retrieved from STRING database.

3.2 Graph convolution-based feature extraction

Having constructed the relevant networks we next extract informative node representations using the node neighborhood information. As we have no input node features, we train embedding layers (of dimension 32) for each of the network.

An embedding layer is essentially a look-up table where i th row corresponds to the learnt representation of i th node. The node embedding is then passed as an input feature to the graph convolutional layer. A graph convolutional layer is essentially a linear layer which transforms the node feature as an aggregation of representations of its 1-hop neighbors. In particular for input adjacency matrix A and

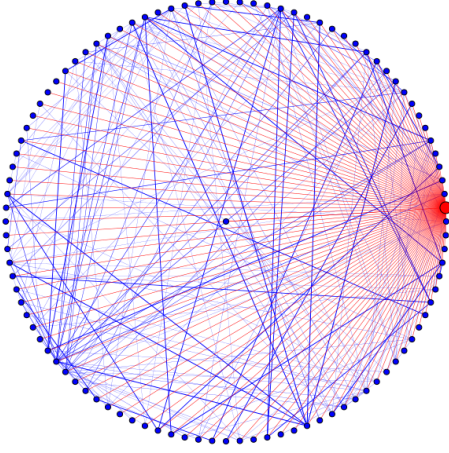


Fig. 4. An illustration of miRNA-PCG, PCG-PCG interactions. Red nodes and red edges denote miRNAs and miRNA-PCG connections while blue nodes and blue edges represent PCGs and PCG-PCG interactions, respectively.

node embedding matrix \mathbf{X} we obtain transformed node feature matrix \mathbf{X}' as follows

$$\mathbf{X}' = \hat{\mathbf{D}}^{-1/2} \hat{\mathbf{A}} \hat{\mathbf{D}}^{-1/2} \mathbf{X} \mathbf{W}, \quad (1)$$

where $\hat{\mathbf{A}} = \mathbf{A} + \mathbf{I}$, \mathbf{I} is the identity matrix and $\hat{\mathbf{D}}$ is the degree matrix of $\hat{\mathbf{A}}$ and \mathbf{W} is trainable weight matrix of the graph convolutional layer. We point out that we don't use any non-linear activations in this module, and the aggregation operation in Equation (1) can be efficiently carried out using sparse matrix multiplications. Moreover, we avoid the issue of non-interpretability in the feature extraction module, which is usually associated with non-linearities.

As the graph semantics are different for each of the networks, no parameter sharing is employed at this stage. We use three separate graph convolutional layers to extract representations for miRNA, PCG and disease nodes. These learned representation will be fed as input to the multi-task optimization/learning module explained in the next section.

3.3 Multi-task optimization/learning

To effectively utilize information from miRNA-PCG and disease-PCG interactions, we design a multitask objective to train our model. In particular, for miRNA-disease, miRNA-PCG, and disease-PCG pairs, we construct association representations by taking an elementwise product of the corresponding node features. For example, for an miRNA-disease input pair (m, d) denoted by nodes m and d respectively, we obtain the corresponding feature vector representation as

$$\mathbf{x}'_{md} = \mathbf{X}'_m \odot \mathbf{X}'_d$$

where \mathbf{X}'_m and \mathbf{X}'_d correspond to output representations of the corresponding graph convolution layer for nodes m and d respectively.

Using the pairwise representations, we then predict the existence of an association between miRNA and disease; and the confidence score of associations for miRNA-PCG and disease-PCG pairs. In summary, we train our model with multi-task loss functions calculated from these three

supervised tasks and use an adaptive loss balancing technique to combine the three individual loss components dynamically at training time. Details about individual task loss and our optimization strategy are presented in the following sections.

3.3.1 miRNA-disease binary classification task loss (\mathcal{L}_1).

We compute the probability of observing an association between an miRNA-disease input pair (m, d) as:

$$y_{md} = \sigma(\mathbf{w}_{MD}^T \mathbf{x}'_{md}) \quad (2)$$

where \mathbf{w}_{MD} is a learnable weight matrix and $\sigma(x) = \frac{1}{1 + \exp(-x)}$ is the sigmoid function. We use binary cross entropy to calculate the training loss for the miRNA-disease classification module as follows:

$$\mathcal{L}_1 = \sum_{m,d} -z_{md} \log y_{md} - (1 - z_{md}) \log(1 - y_{md}) \quad (3)$$

where z_{md} denote the target label known for the corresponding training pair.

3.3.2 miRNA-PCG regression task loss (\mathcal{L}_2).

For an input miRNA-PCG pair (m, p) , we compute the association confidence score as:

$$y_{mp} = \sigma(\mathbf{w}_{MP}^T \mathbf{x}'_{mp}) \quad (4)$$

where \mathbf{w}_{MP} is a learnable weight matrix and $\sigma(x)$ is the sigmoid function. We use the sum of squared error to calculate the training loss for the miRNA-PCG regression module as follows:

$$\mathcal{L}_2 = \sum_{m,p} (y_{mp} - z_{mp})^2, \quad (5)$$

where z_{mp} denotes the target confidence score.

3.3.3 disease-PCG regression task loss (\mathcal{L}_3).

Similar to prediction of miRNA-PCG association, we compute for a disease-PCG input pair (d, p) the association confidence score, y_{dp} . \mathcal{L}_3 is then calculated using the sum of squared error as in 5.

$$\mathcal{L}_3 = \sum_{d,p} (y_{dp} - z_{dp})^2, \quad (6)$$

where z_{dp} denotes the target confidence score.

3.3.4 Multi-Task optimization

We define the final loss for our model as the linear combination of three losses as follows:

$$\mathcal{L} = \mathcal{L}_1 + \alpha_2 \mathcal{L}_2 + \alpha_3 \mathcal{L}_3, \quad (7)$$

where α_2 , and α_3 are the loss weight for the two side tasks. Generally, multi-task networks are difficult to train. Finding the optimal combination of individual task losses is challenging and problem-specific. A task that is too dominant during training will overwhelm the update signals and prevent the network parameters from converging to robust shared features that are useful across all tasks.

We update α_2 , and α_3 so that the difference between the two side tasks contribution at each time step t is minimized.

More specifically, at each time step t , the values for α_2 , and α_3 are computed dynamically as follows:

$$\alpha_2(t) = \frac{\mathcal{L}_3(t-1)}{\mathcal{L}_1(t-1) + \mathcal{L}_2(t-1) + \mathcal{L}_3(t-1) + 10^{-1}} \quad (8)$$

$$\alpha_3(t) = \frac{\mathcal{L}_2(t-1)}{\mathcal{L}_1(t-1) + \mathcal{L}_2(t-1) + \mathcal{L}_3(t-1) + 10^{-1}} \quad (9)$$

We use Adam optimizer with a learning rate of 10^{-3} to train the multi-task model.

4 EXPERIMENTAL SETUP

4.1 miRNA-disease association datasets

We retrieve the set of miRNA-disease associations from the HMDD v2.0 database [17] and HMDD v3.0 database [20]. As pre-processing steps, we retain only associations for miRNAs and diseases for which the PCG interaction information is available. The filtered data for the HMDD v2.0 database, which from now on is denoted as HMDD2, contains 2,303 known associations between 368 miRNA and 124 diseases. The filtered data for the HMDD v3.0 database, which from now on is referred to as HMDD3, includes 8,747 known associations between 710 miRNAs and 311 diseases.

TABLE 1

The data statistics where $|E|$, $|V_{miRNA}|$, $|V_{disease}|$ refer to the number of associations/links, miRNAs and diseases respectively.

DATASET	$ E $	$ V_{miRNA} $	$ V_{disease} $
HMDD2	2,303	368	124
HMDD3	8,747	710	311

4.2 miRNA-PCG interaction.

We obtain the miRNA-PCG interactions from the RAIN database [35]. We include only interactions for the PCGs with at least one associated Reactome pathway [36] as these would be biologically more significant. We use all known miRNA-PCG pairs to train the mi-PCG interaction confidence score prediction task and the target variables are set to be the normalized confidence score of the interaction retrieved from the database.

4.3 disease-PCG interaction.

We obtain the disease-PCG associations from the DISEASES database [37]. Here also, we retain only the associations for the PCGs with at least one associated Reactome pathway. As above, we use all known disease-PCG pairs to train the disease-PCG interaction confidence score prediction side task and the target variables are set to be the normalized confidence score of the known associations retrieved from the database.

Table 2 provides statistics of the three biological networks as described in section 3.1 and the two additional datasets described in section 4.2 and 4.3.

TABLE 2

Statistics for datasets with side information. $|E|$ is the number of connections/associations. $|V_m|$, $|V_d|$, and $|V_P|$ are the number of miRNAs, diseases, and PCGs, correspondingly.

NETWORK	$ E $	$ V_m $	$ V_d $	$ V_P $
miRNA-PCG	178,716	714	-	9,236
DISEASE-PCG	144,846	-	312	9,236
miRNA FAMILY (\mathcal{G}_m)	1,354	217	-	-
DISEASE ONTOLOGY (\mathcal{G}_d)	90	-	128	-
PCG-PCG (\mathcal{G}_p)	4,446,583	-	-	9,236

4.4 Our new test sets

For small-size datasets like HMDD2 and HMDD3, 5-fold CV evaluation is limited as the size of the training and testing sets become much smaller. While one can use HMDD2 for training and HMDD3 for testing, such evaluation is limited as there are many overlapping associations in these two datasets. We, therefore, carefully construct the following four independent tests using the HMDD3 dataset. HMDD2 is used as the training set for evaluation with the new test sets. Let **M2** be the set of all miRNA in HMDD2 and **D2** be the set of all diseases in HMDD2. The construction of the four independent test sets is described below.

TABLE 3

Statistics for our new test datasets.

DATASET	$ E $	$ V_{miRNA} $	$ V_{disease} $
HELD-OUT1	2,669	324	110
HELD-OUT2	6,641	692	303
NOVEL-MIRNA	3,575	577	115
NOVEL-DISEASE	5,308	346	295

HELD-OUT1 for transductive testing. To construct our HELD-OUT1 test set we include all miRNA in **M2** and disease nodes in **D2** which are common in HMDD2 and HMDD3. The HELD-OUT1 test set contains only the associations which are present in HMDD3 but not in HMDD2. This is a transductive setting for link/association prediction such that all nodes in the test set are the same as that in the training set. We randomly generate the same number of negative samples from the set of unknown miRNA-disease pairs. Finally, HELD-OUT1 contains 2,669 known associations between 324 miRNAs and 110 diseases.

HELD-OUT2 for inductive testing. We construct the HELD-OUT2 test set by including all miRNA and disease nodes and their known associations that are present in HMDD3 but not in HMDD2. Note that different from HELD-OUT1, HELD-OUT2 might also contain associations corresponding to miRNA and disease nodes which are not present in the training set HMDD2. We randomly generate the same number of negative samples from the set of unknown miRNA-disease pairs. HELD-OUT2 consists of 6,641 known associations between 692 miRNAs and 303 diseases.

NOVEL-MIRNA. We first fix the set of diseases in our test set to those retained from HMDD2, i.e., the set **D2**. Then all known associations that are (i) between diseases in **D2** and any miRNA and (ii) present in HMDD3 but not in HMDD2 are included in the NOVEL-MIRNA test set.

We randomly generate the same number of negative samples from the set of unknown miRNA-disease pairs.

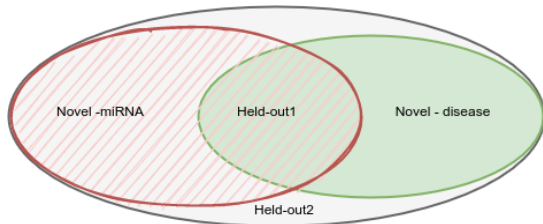


Fig. 5. An illustration of the four large independent test sets relations where $\text{HELD-OUT1} = \text{NOVEL-MIRNA} \cap \text{NOVEL-DISEASE}$, $\text{HELD-OUT2} = \text{NOVEL-MIRNA} \cup \text{NOVEL-DISEASE} = \text{HMDD3} \setminus \text{HMDD2}$.

In the end, our unseen miRNA testing set consists of 3,575 associations between 577 miRNAs and 115 diseases. We use this set to test the performance of models on unseen data where there are new miRNAs for which no prior association is present in the training set.

NOVEL-DISEASE. Similarly, for constructing the NOVEL-DISEASE test set, we first restrict the set of known associations to only those that involve miRNAs in M2. Then we retain only associations that are in HMDD3 but not in HMDD2. We randomly generate the same number of negative samples from the set of unknown miRNA-disease pairs. Finally, we attain 5,308 associations between 346 miRNAs and 295 diseases. We use this set to test the performance of models on unseen data where there are new diseases for which no prior association is present in the training set.

A schematic Venn diagram of the four large independent test sets is presented in Figure 5.

4.5 Benchmarked models

We compare our model with five recently proposed supervised methods. Details about our benchmarked models are given below.

EPMDA [12] EPMDA consists of two components: the feature extractor and the classifier. The feature extraction module adopts a network topology-based approach and operates on a heterogeneous network G . G is constructed from the known miRNA-disease association set, the pre-calculated miRNA, and disease Gaussian Interaction Profile Kernel (GIP) [38] similarities. A Multiple Layer Perceptron (MLP) classifier is employed to do the classification task. EPMDA feature extractor and classifier get trained separately.

NEMII [39] NEMII uses Structural Deep Network Embedding (SDNE) to learn the embedding for miRNA and disease from a bipartite graph built up from known association information. The learned embedding and features extracted from the miRNA family and disease semantic similarity are concatenated to form the input to a Random Forest classifier.

NIMGCN [16] NIMGCN proposes an end-to-end learning framework that operates on a heterogeneous network G , which is built up from miRNA-disease known associations, the pre-calculated miRNA functional similarity (MISIM), and the disease semantic similarities. GCN and non-linear transformation layers are employed to learn the latent representation for miRNAs and diseases separately. For a particular miRNA-disease pair, its association probability is

calculated as the inner product of the two corresponding latent feature vectors.

DBMDA [13]. DBMDA separates the feature learning and classification process. It uses autoencoders to learn the hidden representation for each miRNA-disease pair from pre-calculated similarities as input. The autoencoders are trained in an unsupervised manner. The encoded representation will then be fed as input into a Rotation Forest classifier whose job is to predict potential miRNA-disease associations.

DIMIG 2.0 [15] DIMIG 2.0 is a semi-supervised approach that treats miRNA-disease association prediction as a multiclass classification problem where diseases are the labels. They do not use miRNA-disease association during the training process. Instead, they use only the known disease-PCGs interaction to learn the model parameters. PCGs nodes are connected with miRNAs nodes in a heterogeneous network based on miRNAs interaction profiles. Learned signals are then propagated through the heterogeneous network to infer the labels for miRNAs.

Note that from all the above baselines, only DIMIG 2.0 can be used for testing in inductive settings, i.e., testing for associations/links when the corresponding nodes are not present in the train set.

4.6 Test set-up and evaluation

As in previous works, we perform 5-fold CV for testing on HMDD2 and HMDD3 datasets. We run 5-fold CV with 5 random initializations. In other words, for each dataset, we run each model $5 \times 5 = 25$ times and report the average performance with the standard deviation.

To test on our new test sets, we train the models on the HMDD2 dataset. We run the experiments 5 times with random initializations and report the mean performance scores along with standard deviation. For case studies, we run each model with the given case study data 5 times and report average performance for each model.

Evaluation metrics. Following previous works and recommendations in [19], we report the Area under the Receiver Operating Characteristic (AUC), and Average Precision (AP) as our evaluation criteria. For our case studies, we report the number of known associations found in the top K pairs with the highest prediction scores returned from the model, where k is from 10 to 100 with a step of 10.

4.7 Hyperparameter settings

4.7.1 MuCoMID

In all experiments, we fix the number of training epochs to 200, the embedding size and the hidden dimension both to 32. We employ Adam optimizer with a learning rate of 10^{-3} for training.

4.7.2 Benchmarked models

For EPMDA, DBMDA and NIMGCN, we use the code and setup released in [19]. For NEMII, we use the same code and setup as published by the authors.

For DIMIG 2.0, we use the code and parameters shared by the author. To test the model performance on our data,

we compared DIMIG 2.0 with the input features as tissue expression profiles and DIMIG 2.0 with one-hot vectors on the subset of our testing datasets that have miRNA expression profiles available. The two models acquire similar performance. This implies that use of tissue expression profiles as node features do not have an effect on the model performance. We can therefore test the model on data for which tissue expression information is unavailable by using one hot encoding for input node features. The results reported in Section 5 corresponds to the model with one-hot vectors as input features on our testing datasets without removing miRNAs that don't have expression profiles.

5 RESULTS

In the following, we discuss the performance gains of our approach (and their implications) on a variety of testing scenarios and new test datasets described in sections 4.1 and 4.4.

5.1 Results on small test sets

Following previous works, we perform 5-fold CV experiments on HMDD2 and HMDD3 datasets. The results are shown in Table 4. The test set size for this scenario is considerably smaller and contains only 1/5th of the total associations. The test size is then considerably smaller for datasets like HMDD2. Such a train-test scenario allows us to quantify how well the models learn but is limited in testing the generalization power of the models.

While the graph-based approaches EPMDA and NIMGCN perform reasonably well in this scenario, our multi-task-based approaches significantly supersede state-of-the-art (SOTA) methods with an improvement of up to $\sim 13.8\%$ in AP score.

The performance of EPMDA drops considerably for HMDD3 dataset. EPMDA learns edge features in an unsupervised manner corresponding to its contribution to a cycle of a particular length. Usually, the cycle length parameter is fixed to a small value due to an exponential increase in run time with an increase in cycle length. Moreover, the task signal is not used in learning the edge features. The loss of performance of EPMDA in HMDD3 can be attributed to the limitation of finding the best cycle length hyperparameter applicable for HMDD3. This also limits the applicability of this model to a larger variety of datasets. NIMGCN performs better than DBMDA due to the higher representational capacity of used GCNs and exploitation of additional graph structure.

5.2 Results on small train but larger test sets in transductive setting

Table 5 shows results corresponding to HELD-OUT1 test set. Recall that HMDD2 is used as the training set. In this scenario, the test size is much larger than the train set size allowing us to compare the generalization capability of the models.

Out of the state-of-the-art models, NIMGCN is the best owing to the use of GCNs to extract latent representations. The overall drop in performance of all models in this scenario as compared to small test size case points to the

hardness of this particular test set. Existing methods show a bad generalization capability.

Though both MUCOMID and NIMGCN employ GCNs to extract latent representations, we still observe a significant difference between the two models' performance. The reason for such difference are: (i) NIMGCN is a single task-based model which relies on pre-calculated secondary features and learns solely from the set of known associations while (ii) MUCOMID is a multitask-based model which can incorporate information from five additional knowledge sources to learn the feature automatically at run time and to overcome the limited training data problem.

5.3 Results on small train but larger test sets in inductive setting

Table 6 shows results corresponding to testing on HELD-OUT2 dataset and training on HMDD2. Note that HELD-OUT2 is more than three times larger than the training data and contains new nodes that have not been seen in HMDD2. EPMDA, DBMDA, NIMGCN, and NEMII rely on the known miRNA-disease associations to calculate similarities or learn structural embedding for miRNA and disease. Therefore, they cannot be compared in the current inductive setting with new miRNAs or new diseases.

For such large testing set with many new nodes, MUCOMID still claims its superior performance. With respect to AP score, MUCOMID shows an improvement of $\sim 42.4\%$ over DIMIG 2.0.

This dataset further supports the importance of the chosen architecture and the effectiveness of multi-sources data integration.

5.4 Results on NOVEL-DISEASE and NOVEL-MIRNA datasets

Table 6 shows results with NOVEL-DISEASE and NOVEL-MIRNA test sets. EPMDA, DBMDA, NIMGCN, and NEMII cannot be used for inductive setting with new nodes.

MUCOMID again outperforms its competitor, the DIMIG 2.0 model. The gain is more significant on NOVEL-MIRNA datasets with a gain of $\sim 48.5\%$ in AP score. On NOVEL-DISEASE test set, MUCOMID is $\sim 35.3\%$ better in AP score than DIMIG 2.0.

MUCOMID and DIMIG 2.0 share some design similarities as (i) both use GCNs to learn the node representation from the input graph (ii) both incorporate information from the disease ontology, miRNA-PCG, disease-PCG and PCG-PCG interaction information. However, there are major differences among the two approaches which dictate the differences in their performance. Firstly, MUCOMID use multiple GCNs to learn the representations for miRNA, disease, and PCG separately from different input graphs while DIMIG 2.0 has a single GCN layer to learn the representation for miRNA and PCG from a network build up from PCG-PCG and miRNA-PCG interactions while ignoring the heterogeneous character of the network. Secondly, DIMIG 2.0 formulates the miRNA-disease association prediction as a multi-label node classification problem and DIMIG 2.0 does not use known miRNA-disease associations to train the model; while MUCOMID is a *supervised* multitask model

TABLE 4

Results with 5FoldCV over the HMDD2 and HMDD3 datasets. We perform 5-Fold CV 5 times with different random seeds. We report the average over 25 scores along with standard deviation. Our improvements over state-of-the-art (SOTA) methods are statistically significant with a p-value less than 0.002 on HMDD2 and less than 10^{-30} on HMDD3 datasets.

Method	HMDD2		HMDD3	
	AUC	AP	AUC	AP
EPMDA ([12])	0.744 ± 0.019	0.783 ± .017	0.520 ± 0.011	0.594 ± 0.010
NIMGCN ([16])	0.785 ± 0.018	0.803 ± 0.015	0.795 ± 0.021	0.800 ± 0.018
DBMDA ([13])	0.553 ± 0.019	0.537 ± 0.015	0.749 ± 0.010	0.696 ± 0.009
NEMII ([39])	0.499 ± 0.019	0.502 ± 0.020	0.512 ± 0.008	0.509 ± 0.006
DIMIG 2.0 ([15])	0.493 ± 0.018	0.485 ± 0.012	0.516 ± 0.006	0.508 ± 0.005
MuCOMiD (OURS)	0.833 ± 0.012	0.832 ± 0.015	0.915 ± 0.004	0.910 ± 0.006
Improvement over SOTA	6.1%	3.6%	15.1%	13.8%

TABLE 5

Results on the HELD-OUT1 dataset after five runs. Our improvements over SOTA methods are statistically significant with a p-value less than 10^{-15} .

Method	AUC	AP
EPMDA	0.562 ± 0.085	0.511 ± 0.064
NIMGCN	0.676 ± 0.009	0.642 ± 0.006
DBMDA	0.545 ± 0.011	0.521 ± 0.009
NEMII	0.504 ± 0.002	0.501 ± 0.000
DIMIG 2.0	0.429 ± 0.002	0.471 ± 0.003
MuCOMiD (ours)	0.705 ± 0.005	0.691 ± 0.006
Improvement over SOTA	4.3%	7.6%

that formulate the miRNA-disease association prediction as a binary classification problem.

Finally, a major difference between the two methods is that DIMIG 2.0 can only work for miRNA and disease for which there exist at least one known association with any PCG. MuCOMiD does not suffer from such a problem and can work for any set miRNA and diseases.

5.5 Ablation study

We conduct ablation study to analyze the contribution of additional tasks. The single task baseline employs similar architecture as that of MuCOMiD but without the miRNA-PCG and disease-PCG interaction confidence score prediction side tasks. In other words, it also learns miRNA and disease representation from the miRNA family and the disease ontology networks, respectively. However, they only have one classifier layer for the miRNA-disease association prediction task, instead of one classifier and two regressors as that of MuCOMiD.

Table 7 presents the results for MuCOMiD and its single-task variant on both 5-FoldCV and independent testing set up. MuCOMiD consistently out-perform its single-task baseline in all datasets. The difference is more significant on the large independent testing sets, especially in HELD-OUT1 and NOVEL-MIRNA. These improvements account for the contribution of the two added side tasks. Since PCGs are the most important link between miRNAs and their associated diseases [30], miRNA-PCG and disease-PCG prediction tasks also bring additional insights into the miRNA-disease association prediction problem.

6 CASE STUDIES

To further demonstrate our multi-task model’s predictive capability, we evaluate the model for three specific diseases: BREASTCANCER, PANCREATICCANCER, and DIABETESMELLITUS-type 2. By constructing these case studies, we showcase our model’s predictive performance in predicting associations for a specific new disease. To do that, for a specific disease d , we select the pairs associated with d from the HMDD3 to use as the testing set. The remaining pairs in HMDD3 are used as the training data. We do negative sampling for both the training and testing set so that the number of positive and negative samples in both training and testing sets are equal. For the test set, the negative pairs are generated only corresponding to the disease d . The dataset statistics for our case studies are presented in table 8 where we use the disease names to denotes our generated dataset for that particular disease case study.

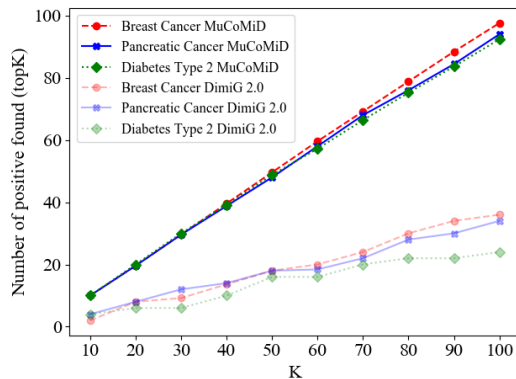


Fig. 6. topK interactions for case studies. Mean number of interactions found over 5 independent runs of the models are reported.

Figure 6 presents the topK evaluation results while table 9 shows the top 50 predictions of the associated miRNAs for the three diseases. For each case study, the known association for that particular disease is completely hidden from the model training process. The statistics of our training and testing data can be found in Section 8.

Looking at Figure 6, though the case studies’ diseases are completely new, our model still attains near-perfect prediction for the top 40 predictions. Compared with DIMIG 2.0 for the top 50 predictions, our model has a gain of at least 166%.

TABLE 6

Results on large test sets with new miRNA and disease after five runs. Our improvements over SOTA methods are statistically significant with a p-value less than 10^{-15} . All models are trained on HMDD2 dataset.

Method	NOVEL-MIRNA		NOVEL-DISEASE		HELD-OUT2	
	AUC	AP	AUC	AP	AUC	AP
DIMIG 2.0	0.452 ± 0.001	0.480 ± 0.001	0.421 ± 0.001	0.467 ± 0.001	0.417 ± 0.003	0.465 ± 0.004
MuCOMiD	0.726 ± 0.005	0.713 ± 0.006	0.637 ± 0.019	0.632 ± 0.025	0.648 ± 0.019	0.662 ± 0.025
Improvement over SOTA	60.6%	48.5%	51.3%	35.3%	55.4%	42.4%

TABLE 7

Ablation study results for both 5-FoldCV and independent testing set up.

Method	MuCOMiD		SINGLE TASK MuCOMiD	
	AUC	AP	AUC	AP
HMDD2	0.833 ± 0.012	0.832 ± .015	0.827 ± 0.009	0.826 ± 0.011
HMDD3	0.915 ± 0.004	0.910 ± 0.006	0.911 ± 0.004	0.906 ± 0.006
HELD-OUT1	0.705 ± 0.005	0.691 ± 0.006	0.667 ± 0.008	0.659 ± 0.007
NOVEL-MIRNA	0.726 ± 0.005	0.714 ± 0.006	0.671 ± 0.008	0.678 ± 0.006
NOVEL-DISEASE	0.637 ± 0.019	0.632 ± 0.025	0.603 ± 0.015	0.616 ± 0.001
HELD-OUT2	0.648 ± 0.019	0.662 ± 0.025	0.603 ± 0.015	0.653 ± 0.010

TABLE 8

Our case studies' datasets' statistics, where n^+ and n^- refer to the number of positive and negative associations/links, respectively.

DISEASE	TRAIN SAMPLES		TRAIN SAMPLES	
	n^+	n^-	n^+	n^-
BREASTCANCER	8423	8423	324	324
PANCREATICCANCER	8578	8578	169	169
DIABETESMELLITUS	8640	8640	107	107

For BREASTCANCER, the model acquires $\sim 97.6\%$ accuracy for the top 100 predictions. For DIABETESMELLITUS-type 2, the number of known positive associations is only 107, but out of the top 100 predictions, we can correctly recognize 92.4 associations (this number is the average of the number of found interactions over five runs). These results again claim the effectiveness of our model in predicting potential associations for new diseases.

7 CONCLUSION

We propose a multi-task graph convolutional learning framework, MuCOMiD for the problem of predicting miRNA-disease associations. Our end-to-end learning approach allows automatic feature extraction while incorporating knowledge from five heterogeneous biological information sources. Incorporating many sources of information helps compensate for the lack of information in any single source and, at the same time, enables the model to generate predictions for any new miRNA or disease. Unlike previous works, our model can be employed in both transductive and inductive settings. To test the generalization power of models, we construct and test on both existing benchmarked set up and on larger independent test sets. Large-scale experiments in several testing scenarios highlight the superiority of our approach. An ablation study is added to highlight the side tasks' contribution. We release all the code and data used in this study for reproducibility and future research at <https://git.l3s.uni-hannover.de/dong/cmtt>.

We believe that our design principles will be of independent interest for other biomedical applications where

data scarcity is a major challenge. In particular, the use of multi-task learning to integrate information from heterogeneous information sources to overcome the problems of data scarcity and unreliability of one single data type is a unique perspective and has not been studied for computational problems in biomedicine.

ACKNOWLEDGMENTS

The work is partially supported by the PRESENT project funded by Volkswagen Stiftung and the State Government of Lower Saxony (grant no. 11-76251-99-3/19 (ZN3434)), the Federal Ministry of Education and Research (BMBF), Germany under the LeibnizKILabor project (grant no. 01DD20003), and the strategic funds of the Translational Alliance in Lower Saxony.

REFERENCES

- [1] J. S. Mattick and I. V. Makunin, "Small regulatory rnas in mammals," *Human molecular genetics*, vol. 14, no. suppl_1, pp. R121–R132, 2005.
- [2] V. N. Kim and J.-W. Nam, "Genomics of microrna," *TRENDS in Genetics*, vol. 22, no. 3, pp. 165–173, 2006.
- [3] H. K. Saini, S. Griffiths-Jones, and A. J. Enright, "Genomic analysis of human microrna transcripts," *Proceedings of the National Academy of Sciences*, vol. 104, no. 45, pp. 17719–17724, 2007.
- [4] Y. Cai, X. Yu, S. Hu, and J. Yu, "A brief review on the mechanisms of mirna regulation," *Genomics, proteomics & bioinformatics*, vol. 7, no. 4, pp. 147–154, 2009.
- [5] M. W. de Ronde, J. M. Ruijter, P. D. Moerland, E. E. Creemers, and S.-J. Pinto-Sietsma, "Study design and qpcr data analysis guidelines for reliable circulating mirna biomarker experiments: a review," *Clinical chemistry*, vol. 64, no. 9, pp. 1308–1318, 2018.
- [6] W. Usuba, F. Urabe, Y. Yamamoto, J. Matsuzaki, H. Sasaki, M. Ichikawa, S. Takizawa, Y. Aoki, S. Niida, K. Kato *et al.*, "Circulating mirna panels for specific and early detection in bladder cancer," *Cancer science*, vol. 110, no. 1, pp. 408–419, 2019.
- [7] F. Jin, H. Hu, M. Xu, S. Zhan, Y. Wang, H. Zhang, and X. Chen, "Serum microrna profiles serve as novel biomarkers for autoimmune diseases," *Frontiers in immunology*, vol. 9, p. 2381, 2018.
- [8] A. Keller, P. Leidinger, A. Bauer, A. ElSharawy, J. Haas, C. Backes, A. Wendschlag, N. Giese, C. Tjaden, K. Ott *et al.*, "Toward the blood-borne mirnome of human diseases," *Nature methods*, vol. 8, no. 10, pp. 841–843, 2011.

TABLE 9

MicroRNAs predicted corresponding to top 50 highest prediction scores produced by MuCoMID (average after 5 runs) for the three case studies.

No.	BREASTCANCER		PANCREATICCANCER		DIABETESMELLITUS-type 2	
1.	hsa-mir-21	0.955	hsa-mir-21	0.956	hsa-mir-21	0.958
2.	hsa-mir-155	0.943	hsa-mir-146a	0.941	hsa-mir-155	0.951
3.	hsa-mir-146a	0.938	hsa-mir-155	0.936	hsa-mir-146a	0.947
4.	hsa-mir-145	0.931	hsa-mir-146b	0.933	hsa-mir-29b	0.938
5.	hsa-mir-29b	0.925	hsa-mir-29b	0.912	hsa-mir-145	0.935
6.	hsa-mir-146b	0.921	hsa-mir-126	0.911	hsa-mir-126	0.918
7.	hsa-mir-126	0.915	hsa-mir-145	0.907	hsa-mir-34a	0.911
8.	hsa-mir-34b	0.89	hsa-mir-210	0.872	hsa-mir-142	0.903
9.	hsa-mir-150	0.889	hsa-mir-150	0.871	hsa-mir-221	0.902
10.	hsa-mir-34a	0.887	hsa-mir-34a	0.87	hsa-mir-150	0.897
11.	hsa-mir-142	0.885	hsa-mir-142	0.867	hsa-mir-34c	0.896
12.	hsa-mir-34c	0.882	hsa-mir-223	0.862	hsa-mir-223	0.889
13.	hsa-mir-210	0.881	hsa-mir-34c	0.857	hsa-mir-122	0.886
14.	hsa-mir-223	0.87	hsa-mir-34b	0.856	hsa-mir-222	0.869
15.	hsa-mir-221	0.868	hsa-mir-122	0.835	hsa-mir-26a	0.864
16.	hsa-mir-122	0.862	hsa-mir-206	0.83	hsa-mir-205	0.862
17.	hsa-mir-205	0.859	hsa-mir-221	0.813	hsa-mir-29a	0.853
18.	hsa-mir-31	0.857	hsa-mir-31	0.811	hsa-mir-375	0.85
19.	hsa-mir-206	0.835	hsa-mir-143	0.809	hsa-mir-144	0.848
20.	hsa-mir-144	0.832	hsa-mir-205	0.805	hsa-mir-143	0.846
21.	hsa-mir-29a	0.832	hsa-mir-375	0.802	hsa-mir-206	0.844
22.	hsa-mir-143	0.83	hsa-mir-222	0.795	hsa-mir-27b	0.831
23.	hsa-mir-124	0.828	hsa-mir-26a	0.794	hsa-mir-24	0.83
24.	hsa-mir-26a	0.827	hsa-mir-183	0.785	hsa-mir-192	0.826
25.	hsa-mir-222	0.822	hsa-mir-181a	0.785	hsa-mir-183	0.824
26.	hsa-mir-375	0.821	hsa-mir-24	0.782	hsa-mir-27a	0.819
27.	hsa-mir-183	0.818	hsa-mir-29a	0.776	hsa-mir-19b	0.816
28.	hsa-mir-24	0.811	hsa-mir-22	0.748	hsa-mir-1	0.813
29.	hsa-mir-132	0.807	hsa-mir-19a	0.743	hsa-mir-214	0.808
30.	hsa-mir-1	0.797	hsa-mir-20a	0.742	hsa-mir-9	0.807
31.	hsa-mir-192	0.796	hsa-mir-204	0.74	hsa-mir-19a	0.802
32.	hsa-mir-19b	0.795	hsa-mir-29b-1	0.738	hsa-mir-17	0.798
33.	hsa-mir-29b-1	0.793	hsa-mir-106b	0.735	hsa-mir-20a	0.798
34.	hsa-mir-29c	0.792	hsa-mir-29c	0.735	hsa-mir-92a	0.797
35.	hsa-mir-181a	0.79	hsa-mir-17	0.734	hsa-mir-22	0.797
36.	hsa-mir-27b	0.789	hsa-mir-106a	0.734	hsa-mir-93	0.795
37.	hsa-mir-196a	0.785	hsa-mir-18a	0.732	hsa-mir-182	0.792
38.	hsa-mir-182	0.78	hsa-mir-132	0.727	hsa-mir-18a	0.792
39.	hsa-mir-19a	0.78	hsa-mir-182	0.722	hsa-mir-132	0.791
40.	hsa-mir-22	0.779	hsa-mir-18b	0.717	hsa-mir-18b	0.788
41.	hsa-mir-17	0.777	hsa-mir-19b-1	0.705	hsa-mir-20b	0.785
42.	hsa-mir-20a	0.777	hsa-mir-27b	0.698	hsa-mir-23b	0.785
43.	hsa-mir-9	0.776	hsa-mir-16	0.688	hsa-mir-486	0.782
44.	hsa-mir-92a	0.774	hsa-mir-15a	0.688	hsa-mir-15a	0.775
45.	hsa-mir-15a	0.773	hsa-mir-92a	0.686	hsa-mir-195	0.771
46.	hsa-mir-214	0.772	hsa-mir-342	0.683	hsa-mir-204	0.767
47.	hsa-mir-106b	0.771	hsa-mir-214	0.682	hsa-mir-320a	0.766
48.	hsa-mir-29b-2	0.769	hsa-mir-133b	0.68	hsa-mir-23a	0.757
49.	hsa-mir-16	0.769	hsa-mir-9	0.678	hsa-mir-15b	0.749
50.	hsa-mir-93	0.768	hsa-mir-96	0.673	hsa-mir-133b	0.749

- [9] R. Schickel, B. Boyerinas, S. Park, and M. Peter, "MicroRNAs: key players in the immune system, differentiation, tumorigenesis and cell death," *Oncogene*, vol. 27, no. 45, pp. 5959–5974, 2008.
- [10] W. Zhang, J. E. Dahlberg, and W. Tam, "MicroRNAs in tumorigenesis: a primer," *The American journal of pathology*, vol. 171, no. 3, pp. 728–738, 2007.
- [11] Y. Lin, Y. Zeng, F. Zhang, L. Xue, Z. Huang, W. Li, and M. Guo, "Characterization of microRNA expression profiles and the discovery of novel microRNAs involved in cancer during human embryonic development," *PloS one*, vol. 8, no. 8, p. e69230, 2013.
- [12] Y. Dong, Y. Sun, C. Qin, and W. Zhu, "Epmda: Edge perturbation based method for mirna-disease association prediction," *IEEE/ACM Transactions on Computational Biology and Bioinformatics*, 2019.
- [13] K. Zheng, Z.-H. You, L. Wang, Y. Zhou, L.-P. Li, and Z.-W. Li, "Dbmda: A unified embedding for sequence-based mirna similarity measure with applications to predict and validate mirna-disease associations," *Molecular Therapy-Nucleic Acids*, vol. 19, pp. 602–611, 2020.
- [14] M. Liu, J. Yang, J. Wang, and L. Deng, "Predicting mirna-disease associations using a hybrid feature representation in the heterogeneous network," *BMC Medical Genomics*, vol. 13, no. 10, pp. 1–11, 2020.
- [15] X. Pan and H.-B. Shen, "Scoring disease-microRNA associations by integrating disease hierarchy into graph convolutional networks," *Pattern Recognition*, p. 107385, 2020.
- [16] J. Li, S. Zhang, T. Liu, C. Ning, Z. Zhang, and W. Zhou, "Neural inductive matrix completion with graph convolutional networks for mirna-disease association prediction," *Bioinformatics*, 2020.
- [17] Y. Li, C. Qiu, J. Tu, B. Geng, J. Yang, T. Jiang, and Q. Cui, "Hmdd v2. 0: a database for experimentally supported human microRNA and disease associations," *Nucleic acids research*, vol. 42, no. D1, pp. D1070–D1074, 2014.
- [18] D. Wang, J. Wang, M. Lu, F. Song, and Q. Cui, "Inferring the human microRNA functional similarity and functional network based on microRNA-associated diseases," *Bioinformatics*, vol. 26, no. 13, pp. 1644–1650, 2010.
- [19] T. N. Dong and M. Khosla, "Towards a consistent evaluation of mirna-disease association prediction models," in *2020 IEEE International Conference on Bioinformatics and Biomedicine (BIBM)*.

- IEEE, 2020, pp. 1835–1842.
- [20] Z. Huang, J. Shi, Y. Gao, C. Cui, S. Zhang, J. Li, Y. Zhou, and Q. Cui, “Hmdd v3.0: a database for experimentally supported human miRNA–disease associations,” *Nucleic acids research*, vol. 47, no. D1, pp. D1013–D1017, 2019.
- [21] E. M. Small, R. J. Frost, and E. N. Olson, “MicroRNAs add a new dimension to cardiovascular disease,” *Circulation*, vol. 121, no. 8, pp. 1022–1032, 2010.
- [22] Z. Yang, L. Wu, A. Wang, W. Tang, Y. Zhao, H. Zhao, and A. E. Teschendorff, “dbdemc 2.0: updated database of differentially expressed miRNAs in human cancers,” *Nucleic acids research*, vol. 45, no. D1, pp. D812–D818, 2017.
- [23] X. Chen, M.-X. Liu, and G.-Y. Yan, “Rwrmda: predicting novel human miRNA–disease associations,” *Molecular BioSystems*, vol. 8, no. 10, pp. 2792–2798, 2012.
- [24] G. Li, J. Luo, Q. Xiao, C. Liang, and P. Ding, “Predicting miRNA–disease associations using label propagation based on linear neighborhood similarity,” *Journal of biomedical informatics*, vol. 82, pp. 169–177, 2018.
- [25] X. Chen, D.-H. Zhang, and Z.-H. You, “A heterogeneous label propagation approach to explore the potential associations between miRNA and disease,” *Journal of translational medicine*, vol. 16, no. 1, p. 348, 2018.
- [26] X. Zeng, W. Wang, G. Deng, J. Bing, and Q. Zou, “Prediction of potential disease-associated miRNAs by using neural networks,” *Molecular Therapy-Nucleic Acids*, vol. 16, pp. 566–575, 2019.
- [27] B.-Y. Ji, Z.-H. You, L. Cheng, J.-R. Zhou, D. Alghazzawi, and L.-P. Li, “Predicting miRNA–disease association from heterogeneous information network with graph embedding model,” *Scientific Reports*, vol. 10, no. 1, pp. 1–12, 2020.
- [28] T. N. Kipf and M. Welling, “Semi-supervised classification with graph convolutional networks,” in *International Conference on Learning Representations (ICLR)*, 2017.
- [29] J. J. Rodriguez, L. I. Kuncheva, and C. J. Alonso, “Rotation forest: A new classifier ensemble method,” *IEEE transactions on pattern analysis and machine intelligence*, vol. 28, no. 10, pp. 1619–1630, 2006.
- [30] S. Mørk, S. Pletscher-Frankild, A. Palleja Caro, J. Gorodkin, and L. J. Jensen, “Protein-driven inference of miRNA–disease associations,” *Bioinformatics*, vol. 30, no. 3, pp. 392–397, 2014.
- [31] B. Kaczkowski, E. Torarinsson, K. Reiche, J. H. Havgaard, P. F. Stadler, and J. Gorodkin, “Structural profiles of human miRNA families from pairwise clustering,” *Bioinformatics*, vol. 25, no. 3, pp. 291–294, 2009.
- [32] A. Kozomara and S. Griffiths-Jones, “mirbase: integrating miRNA annotation and deep-sequencing data,” *Nucleic acids research*, vol. 39, no. suppl_1, pp. D152–D157, 2010.
- [33] L. M. Schriml, C. Arze, S. Nadendla, Y.-W. W. Chang, M. Mazaitis, V. Felix, G. Feng, and W. A. Kibbe, “Disease ontology: a backbone for disease semantic integration,” *Nucleic acids research*, vol. 40, no. D1, pp. D940–D946, 2012.
- [34] D. Szklarczyk, A. Franceschini, S. Wyder, K. Forslund, D. Heller, J. Huerta-Cepas, M. Simonovic, A. Roth, A. Santos, K. P. Tsafou *et al.*, “String v10: protein–protein interaction networks, integrated over the tree of life,” *Nucleic acids research*, vol. 43, no. D1, pp. D447–D452, 2015.
- [35] A. Junge, J. C. Refsgaard, C. Garde, X. Pan, A. Santos, F. Alkan, C. Anthon, C. von Mering, C. T. Workman, L. J. Jensen *et al.*, “Rain: Rna–protein association and interaction networks,” *Database*, vol. 2017, 2017.
- [36] A. Fabregat, S. Jupe, L. Matthews, K. Sidiropoulos, M. Gillespie, P. Garapati, R. Haw, B. Jassal, F. Korninger, B. May *et al.*, “The reactome pathway knowledgebase,” *Nucleic acids research*, vol. 46, no. D1, pp. D649–D655, 2018.
- [37] S. Pletscher-Frankild, A. Pallejà, K. Tsafou, J. X. Binder, and L. J. Jensen, “Diseases: Text mining and data integration of disease–gene associations,” *Methods*, vol. 74, pp. 83–89, 2015.
- [38] T. van Laarhoven, S. B. Nabuurs, and E. Marchiori, “Gaussian interaction profile kernels for predicting drug–target interaction,” *Bioinformatics*, vol. 27, no. 21, pp. 3036–3043, 2011.
- [39] Y. Gong, Y. Niu, W. Zhang, and X. Li, “A network embedding-based multiple information integration method for the miRNA–disease association prediction,” *BMC bioinformatics*, vol. 20, no. 1, pp. 1–13, 2019.



Ngan Dong is PhD student at L3S Research Center, Leibniz University of Hannover, Germany. She works as a research assistant in the PRESENT project¹, which aims at integrating clinical, biological, and big data research to advance our understanding of norovirus gastroenteritis. Her current research focuses on network analysis, feature selection, graph-based representation learning, multi-task models, and data integration.



Stefanie Mücke received her B. Sc. and M. Sc. in Biology at the Martin-Luther-Universität Halle/Wittenberg (Germany) in 2013 and 2016, respectively. In 2020, she earned her Ph.D. in Biotechnology at the Gottfried Wilhelm Leibniz Universität Hannover (Germany), working on host-pathogen interactions, omics analyses, genetic engineering, and biotechnology. Since 2020, she has been a scientific officer for the Translational Alliance in Lower Saxony, a network of 10 research institutions in Hannover and Braunschweig (Germany). She supports cooperation projects between these institutions in the capacity of a project manager and scientific advisor.



Megha Khosla received her PhD degree in Theoretical Computer Science from Max Planck Institute of Informatics and Saarland University, Saarbruecken, Germany. Currently she is a senior researcher at L3S Research center. Her main research focus is on effective, interpretable and privacy-preserving learning on graphs with applications to personalized medicine.

1. <http://www.translationsallianz.de/train-platforms/train-projects/present/?L=1>